THROUGH WELD INSPECTION OF WROUGHT STAINLESS STEEL PIPING USING PHASED ARRAY ULTRASONIC PROBES

Michael T. Anderson, Stephen E. Cumblidge, Steven R. Doctor
Pacific Northwest National Laboratory, Richland, WA, USA

Abstract: A study was conducted to assess the ability of phased-array ultrasonic techniques to detect and accurately determine the size of flaws from the far-side of wrought austenitic piping welds. The work was sponsored by the U.S. Nuclear Regulatory Commission under Contract DE-AC06-76RLO 1830; NRC JCN Y6604; Ms. Deborah Jackson, Program Monitor. Far-side inspections of these welds are currently performed on a "best effort" basis and do not conform to ASME Code Section XI Appendix VIII performance demonstration requirements. For this study, four circumferential welds in 610mm diameter, 36mm thick ASTM A-358, Grade 304 vintage austenitic stainless steel pipe were examined. The welds were fabricated with varied welding parameters; both horizontal and vertical pipe orientations were used, with air and water backing, to simulate field welding conditions. A series of saw cuts, electro-discharge machined (EDM) notches, and implanted fatigue cracks were placed into the heat affected zones of the welds. The saw cuts and notches range in depth from 7.5% to 28.4% through-wall. The implanted cracks ranged in depth from 5% through wall to 64% through wall. The welds were examined with two phased-array probes, a 2.0 MHz transmit-receive longitudinal wave array and a 2.0 MHz transmit-receive shear wave array. These examinations showed that both phased-array transducers were able to detect and accurately length-size, but not depth size, all of the notches and flaws through the welds. The phased-array results were not strongly affected by the different welding techniques used in each weld.

Introduction: Austenitic steels are used for applications where resistance to corrosion, or high strength and creep resistance are required at elevated temperatures, such as in the primary piping circuit of a light water reactor (LWR). Ultrasonic methods have been routinely used for inservice inspection of nuclear components for several decades and yet, welded austenitic materials remain difficult to reliably and effectively examine using ultrasound. Typically, the austenite phase forms long columnar grains based on the weld bead size and direction of maximum heat loss during solidification and cooling processes [1]. Due to the physical properties of these grains, many inspection problems can arise, and ultrasonic flaw responses are often obscured by scattered energy from the material structure.

Because field welds are normally at terminal ends of piping segments, access to both sides of these welds may be limited due to component configurations, i.e., valves, pumps, or vessels may be connected to these piping runs at the field welds. Thus, development of effective and reliable far-side inspection techniques, as performed from the accessible near-side of the weld, for these field welds is necessary. Far-side austenitic weld inspections continue to perform unsatisfactorily due to the large size and orientation of anisotropic grains which may cause severe attenuation, beam skewing, changes in velocity, and scattering of ultrasonic energy [2]. In addition, refraction and reflection of the sound beam may occur at the grain boundaries, from weld root and counter-bore geometries, and at weld fusion lines, resulting in difficulties in distinguishing flaw responses from those of geometric or metallurgical origin. The use of phased array technology provides the capability to efficiently assess the effect of varied inspection angles and focal lengths on these welds. The purpose of this paper is to present the results of laboratory investigations of commercially-available ultrasonic phased array technologies as applied to the far-side inspection of wrought austenitic piping welds.

Results and Discussion: Laboratory trials for austenitic piping welds used multi-element 2.0 MHz dual arrays, including transmit-receive longitudinal (TRL) wave and transmit-receive shear (TRS) wave probes designed for this study [4]. The arrays were highly damped (bandwidths of 70-80%) and configured to produce beam angles of 30° to 70° in the weld volume, controlled at 1° increments by focal laws, with integral roof and squint angles in the wedge to optimize the focal crossover point in the required thickness range. Each array in the TRL probe has an aperture of 20mm (active) and 10mm (passive). The TRS array

apertures are 32mm by 12mm, active and passive, respectively. Automated line scans oriented parallel to the weld were performed to produce data sets from a range of array-to-weld centerline positions.

The specimen (02-24-15) used for Phase 1 was made with ASTM A-358, Grade 304 vintage austenitic stainless steel piping segments having nominal 610mm outside diameter and approximately 36mm wall thickness. During the welding process several cracks were implanted into the heat-affected zone (HAZ) of the girth weld. In addition to the implanted cracks, eight saw cuts were made into the heat-affected zone of the weld to provide standard ultrasonic reflectors. Descriptive parameters of the cracks and saw cuts used for this study are shown in Tables 1 and 2.

Table 1 - Implanted Cracks in Austenitic Piping Specimen 02-24-15

Crack Designation	A	B	C	D	E
Crack Orientation	Circ.	Circ.	Circ.	Axial	Circ.
Crack Length [±1.0-mm]	10 mm	30 mm	44 mm	13 mm	34 mm
Through-wall Depth [±1.0 mm]	5 mm	15 mm	22 mm	7 mm	17 mm
% Wall Thickness	15	43	64	19	48
Circumferential Location (from 0°)	30°	65°	165°	270°	330°

Table 1 - Saw Cuts in Austenitic Piping Specimen 02-24-15

Designation	A	B	C	D	E	F	G	H
Angle	90°	90°	35°	90°	90°	35°	35°	35°
Length [±0.5mm]	33 mm	65 mm	36 mm	54 mm	44 mm	60 mm	57 mm	68 mm
Depth [±0.5mm]	3 mm	10 mm	3 mm	7 mm	4 mm	7 mm	6 mm	9 mm
% Wall	7.5	28.4	7.1	18.8	12	19	18	26
Location	22.5°	45°	85°	150°	185°	210°	285°	310°

Near- and far-side results for portions of pipe specimen 02-24-15 show that all circumferential cracks and saw cuts are clearly detectable (Figures 1, 2 and 3), however, shallower flaws are more difficult to detect than flaws with features that penetrate further through-wall [4]. No scans parallel to the weld to observe responses from the axial flaw were performed. The TRL array near-side data exhibits strong ID corner-trapped responses, and clear diffracted tip signals. The TRS array data also shows corner trap responses, but weak tip signals, if any, from the near-side. From the far-side of the weld the TRL array performs well in detecting the 35° angle saw cuts while both arrays are able to detect the straight cuts and cracks. Neither array is able to produce detectable tip signals for the defects from the far-side of the weld. This presents a significant challenge for depth-sizing of any detected flaws on the far-side.

Length-sizing of flaws from the far-side of a weld is possible. The saw cuts and implanted cracks were length-sized using a 6dB-drop technique and a loss-of-signal (LOS) technique. As the UT signal from a linear defect is often broken up as it passes through the weld microstructure, the 6dB-drop technique is not as useful as the LOS method. The root-mean-squared (RMS) error for the TRL probe in length-sizing of the flaws from the far-side of the weld was 6.3mm; this is well within the acceptance criteria of ASME XI, Appendix VIII. The RMS error for the TRS probe from the far-side of the weld was 15.3mm, which also meets the ASME acceptance criteria, but is not as accurate as the TRL results. In the absence of tip-diffracted signals, no attempt to perform time-of-flight depth-sizing was made for the data from either probe. Figure 4 shows actual crack and saw-cut lengths plotted against the ultrasonic length-sizing results for both the 6dB-drop and LOS methods. As one would expect, machined reflectors are much more accurately sized than actual cracks.

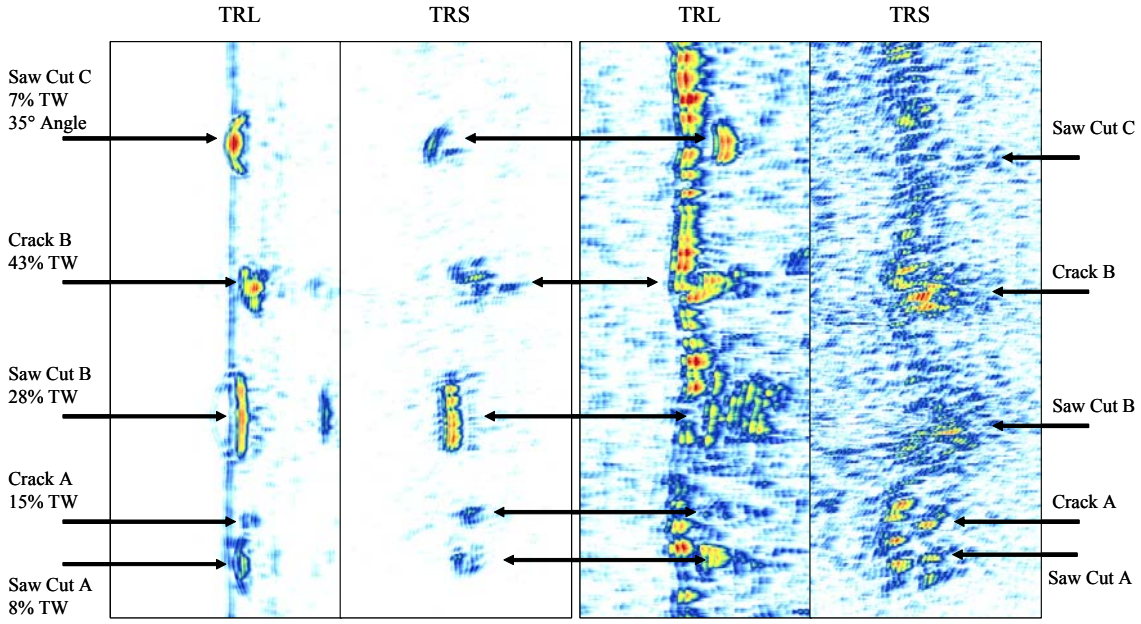

Figure 1 - B-Scan views for specimen 02-24-15, segment 1 from the near- and far-side with TRL and TRS arrays.

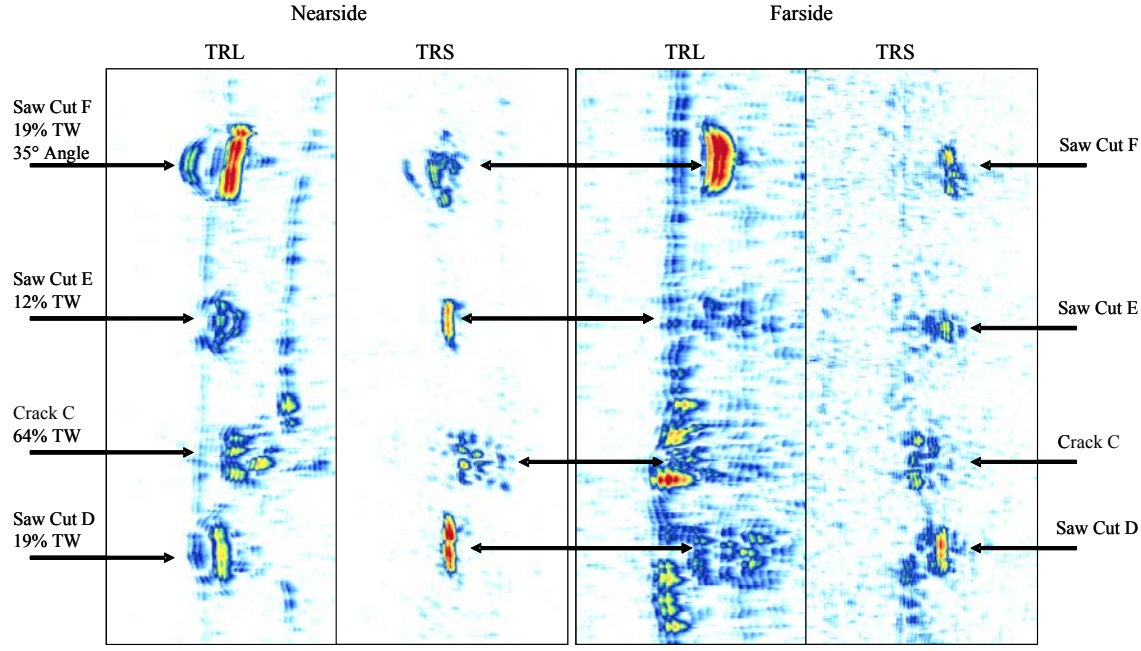

Figure 2 - B-Scan views for specimen 02-24-15, segment 2 from the near- and far-side with TRL and TRS arrays.

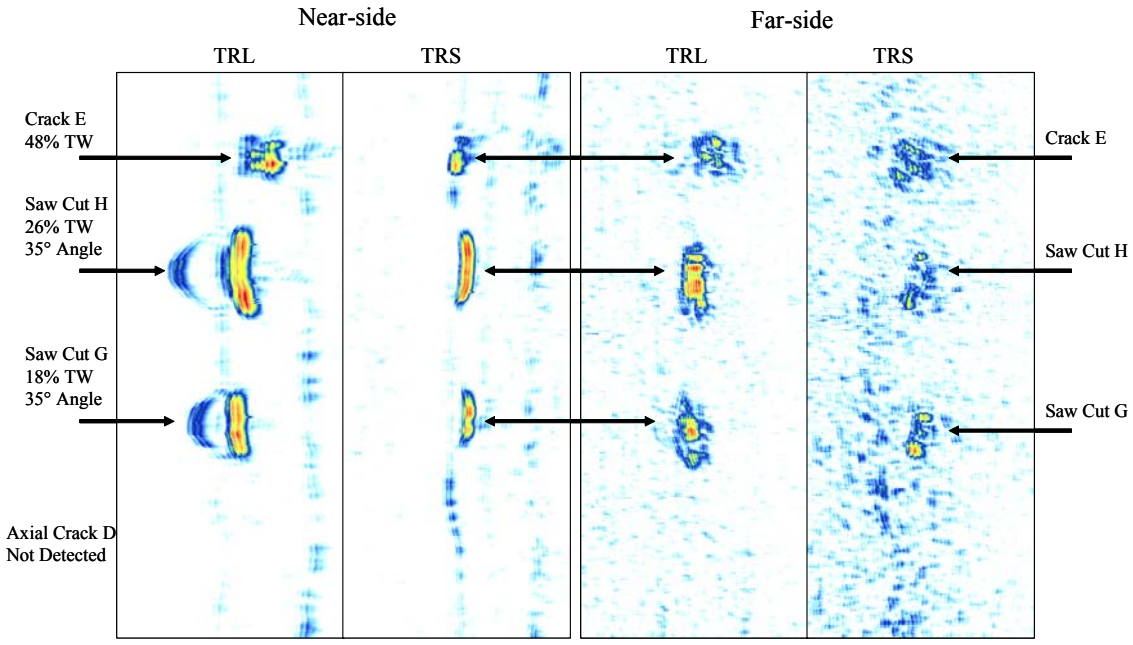

Figure 3 - B-Scan views for specimen 02-24-15, segment 3 from the near- and far-side with TRL and TRS arrays.

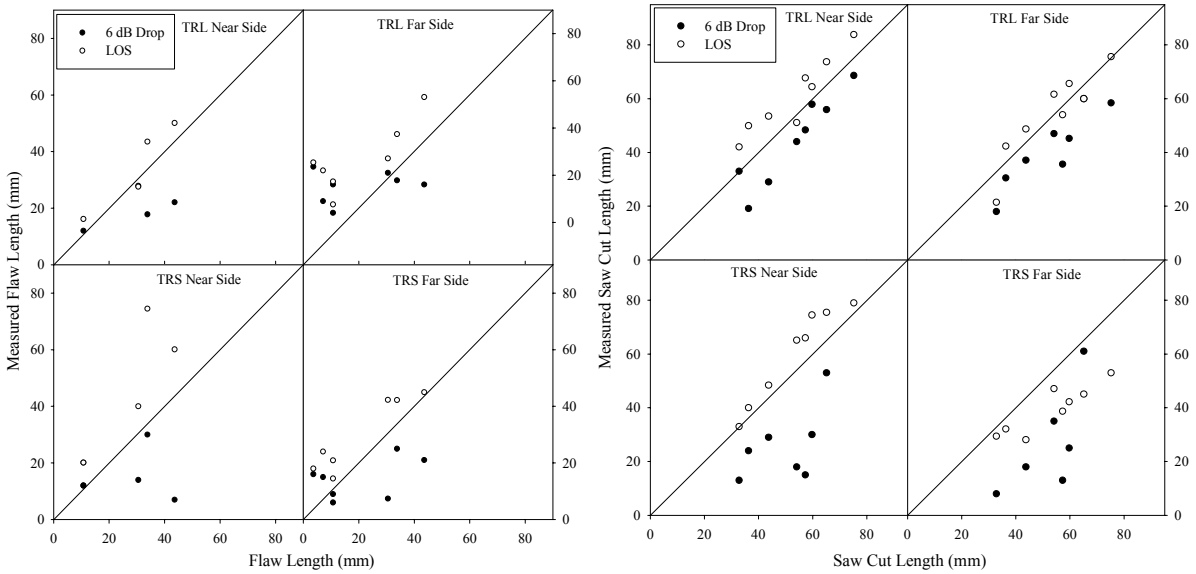

Figure 4 - Length-sizing data for saw cuts and implanted flaws using 6dB drop and LOS methods.

In Phase 2 three welds were examined to determine the effects of weld microstructure on the reliability of far- side inspections. Pipe specimen 3C-022 is made of schedule 80 ASTM 358 Grade 304 wrought stainless steel, and consists of three 610mm diameter pipe sections joined by three welds: 1) horizontally-positioned air-back weld, 2) vertically-positioned air-back weld, and 3) horizontally-positioned water-back weld. A 360°, 10% through-wall notch is machined into the heat-affected zone of these welds to provide a consistent standard reflector. Weld two also contains three implanted cracks of 5%, 10%, and 15% through-wall depth in

the heat-affected zone. These welds were examined using both TRL and TRS arrays. A sample region of the ultrasonic response of the 10% notch is shown in Figure 5. The dead zone near the top of both scans is caused by the longitudinal seam weld in the pipe. The images are shown with the gain set so that the noise level was approximately 20% FSH.

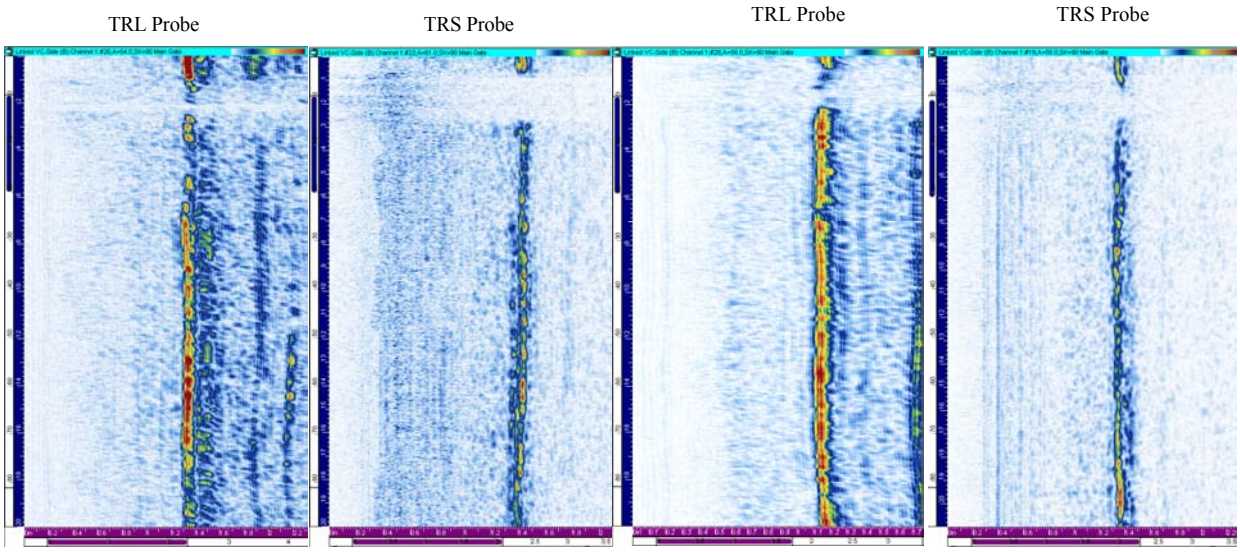

Figure 5 - B-Scan views for ultrasonic responses for the 10% notch in a portion of specimen 3C-022, welds one (left) and three (right) from the far-side with TRL and TRS arrays.

The 360° scans around the pipe specimen showed that while there was strong short-range variability in the strength of the ultrasonic response, there was no overall "structure" to the interference, i.e., the ultrasonic response for the pipe section that was near the top (at the 12 o'clock position and welded down-hand from above) during the welding process is essentially the same as the response near each side and the bottom (at the 6 o'clock position and welded from underneath). However, the amplitude of the ultrasonic response from the 10% though-wall notch was not constant and steady, but instead increased and decreased strongly in the scanning direction. Overall, the TRL array has a better signal-to-noise ratio than the TRS array.

Signal responses varied significantly between the TRL and TRS arrays. Using 44dB of gain with the TRL probe, the peak signal amplitude of the 10% notch from the near-side scan is 100% FSH with a low value of 57% FSH along the notch length. A clear corner response is visible in the scan. At the same gain setting (44dB), the peak response from the far-side is 100% FSH and the lowest signal along the notch length is 40% FSH. Thus, the far-side scan shows a similarly intense signal, but the ultrasonic response from the notch is less discrete than from the near-side. No tip signal responses can be detected in either scan. The results indicate that 2.0 MHz longitudinal waves pass through the weld metal with minimal loss of amplitude, but with much sound field redirection. Typical A-scans, shown in Figure 6, show the differences in the nature of the signal coming back from the EDM notch for the TRL array.

The shear-wave response from the EDM notch was quite different than the longitudinal-wave response. The shear waves were severely attenuated but appear to be less redirected by the weld metal. Using 23dB of gain from the near-side the maximum response is 100% FSH with the minimum response along the EDM notch length being 78% FSH, while at the same gain setting (23dB), the far-side maximum response is 30% FSH with a minimum of 5% FSH. This represents an amplitude drop of 10 to 20dB through the weld. However, the EDM notch response appears more like the response from a linear feature and shows that the shear-wave beam is not redirected as severely as the longitudinal waves. The A-scans shown in Figure 7 indicate that the largest effect on the beam as it passes through the weld metal is the reduction in amplitude. (It should be noted that less gain is needed for the TRS array as it has a larger aperture and there is no loss of energy due to mode conversion on the ID surface as compared to the TRL array.)

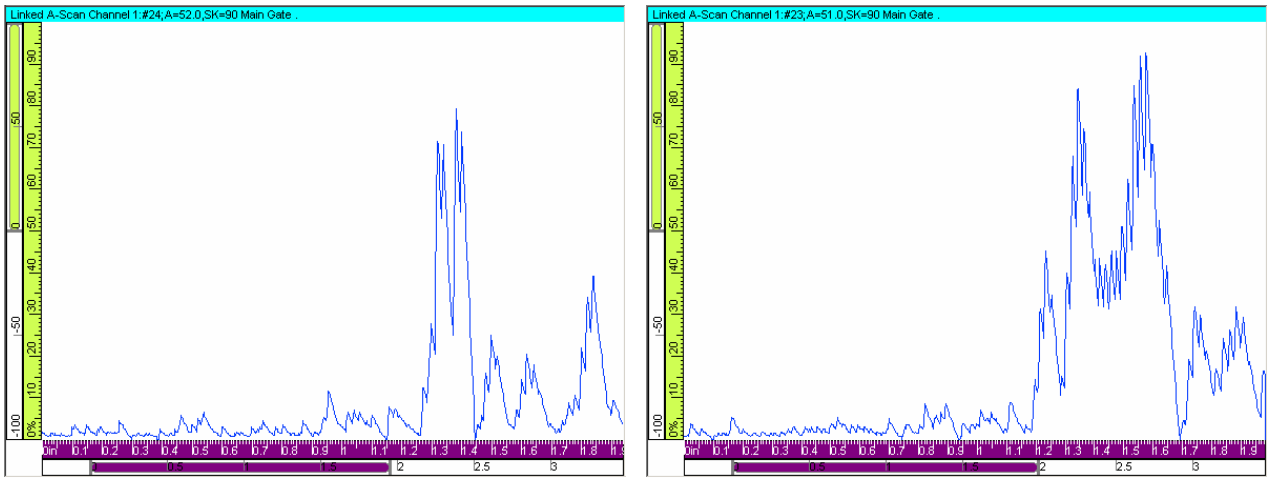

Figure 6 - A-Scan views for the ultrasonic response from an EDM notch along the weld HAZ from the near- (left) and far-side (right) with the longitudinal wave array.

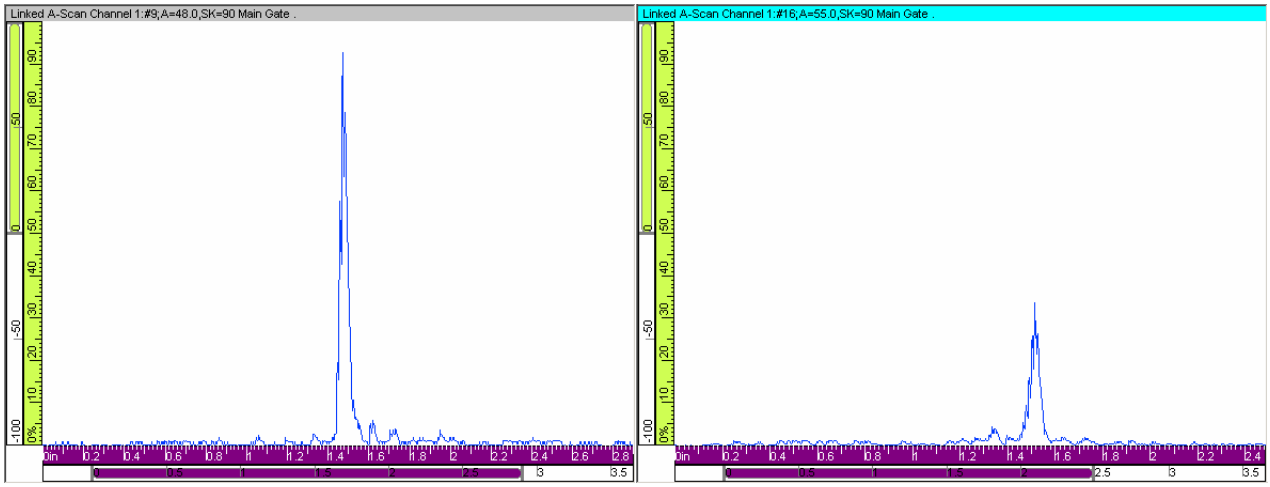

Figure 7 - A-Scan views for the ultrasonic response from an EDM notch along the weld HAZ from the near- (left) and far-side (right) with the shear wave array.

The three implanted flaws are all detectable from the far-side using both the TRL and TRS arrays. Again, no tip signals were detected from the far-side by either array for any of the flaws. Figure 8 depicts the ultrasonic responses from the far-side for the three implanted flaws using the TRL and TRS arrays. The detection of these implanted flaws validate the Phase 1 results, in that, given varied welding microstructures, PA technology is capable of penetrating these weld configurations.

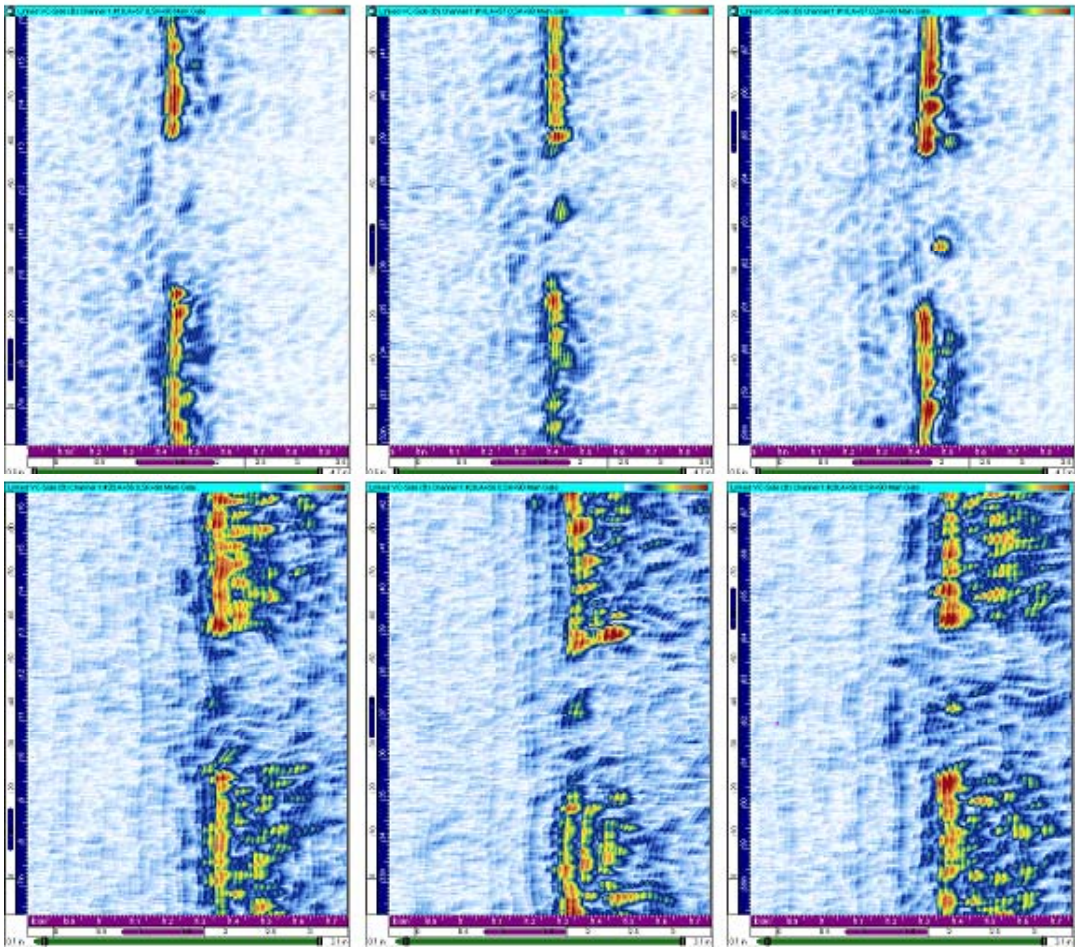

Figure 8 - B-Scan views for ultrasonic responses from three implanted flaws (left-to-right: 5, 10 and 15% through-wall cracks) in weld two from the far-side with the TRS (top) and TRL (bottom) arrays.

Conclusions: The results show that PA technology, using TRL and TRS arrays, is capable of detecting and length-sizing defects from the far-side of welds in wrought austenitic stainless steel piping. All circumferential flaws were detected, although some flaws (<15% through-wall) were difficult to discern from weld root responses. With the TRL array, no corner-trap or tip-diffracted responses were evident from far-side flaws; only spectral reflectors can be used for detection. The TRS array was more effective in detecting the far-side corner trap responses. This may be the result of a better corner trap capability with vertical polarized shear waves and larger aperture of the TRS array, allowing for a more tightly focused beam at higher angles. Neither array could depth-size defects from the far-side of the weld as no crack tip signals could be observed. There was little difference in the ultrasonic responses from standard reflectors with the different welding techniques used on the Phase 2 piping specimen. There was no evidence that suggests that the "down-hand" weld used in the Phase 1 pipe specimen is significantly different from the field-like welds used in Phase 2 pipe. The overall results strongly corroborate initial findings and show validity for field-welded piping. This work has been performed to further enhance the current "best effort" methods for examining the far-side regions of austenitic piping welds, and should promote ASME Code performance demonstration activities for reliable qualification of procedures, personnel, and equipment.

References

1. J. Moysan, A. Apfel, G. Corneloup, B. Chassignole, “Modelling the Grain Orientation of Austenitic Stainless Steel Multipass Welds to Improve Ultrasonic Assessment of Structural Integrity”, International Journal of Pressure Vessels and Piping 80, 77-85, 2003.
2. D. MacDonald, M. Dennis, J. Landrum, and G. Selby. “Phased Array UT Performance on Dissimilar Metal Welds: Interim Report”. EPRI Nondestructive Evaluation Center, Charlotte, North Carolina, 2000. TE-1000116.
3. M. Delaide, G. Maes, D. Verspeelt, “Design and Application of Low-Frequency Twin Side-by-Side Array Transducers for Improved UT Capability on Cast Stainless Steel Components”, Second Int. Conf. on NDE in Relation to Structural Integrity for Nuclear and Pressurized Components, New Orleans, LA, May 2000.
4. M. Anderson, S. Cumblidge, S. Doctor, “Applying Ultrasonic Phased Array Technology to Examine Austenitic Coarse-Grained Structures for Light Water Reactor Piping”, Third EPRI Phased Array Inspection Seminar, Seattle, WA, June 2003.